Colloids and Surfaces B: Biointerfaces 129 (2015) 137–145

Contents lists available at ScienceDirect

Colloids and Surfaces B: Biointerfaces

journal homepage: www.elsevier.com/locate/colsurfb

Reduction-sensitive micelles with sheddable PEG shells self-assembled from a Y-shaped amphiphilic polymer for intracellular doxorubicine release

Can Cui[a,b], Ping Yu[a], Ming Wu[a], Yang Zhang[a], Lei Liu[a], Bo Wu[a], Cai-Xia Wang[a], Ren-Xi Zhuo[a], Shi-Wen Huang[a,*]

[a] Key Laboratory of Biomedical Polymers, Ministry of Education, Department of Chemistry, Wuhan University, Wuhan 430072, PR China
[b] Key Laboratory of High-temperature and High-pressure Study of the Earth's Interior, Institute of Geochemistry, Chinese Academy of Sciences, Guiyang 550002, PR China

ARTICLE INFO

Article history:
Received 22 December 2014
Received in revised form 13 March 2015
Accepted 16 March 2015
Available online 23 March 2015

Keywords:
Y-shaped
Micelle
Reduction-sensitive
Sheddable PEG

ABSTRACT

A new type of shell-sheddable micelles with disulfide linkages between the hydrophobic polyester core and hydrophilic poly(ethylene glycol) (PEG) shell was developed based on Y-shaped amphiphilic polymers mPEG-S-S-$(PCL)_2$. The micelles were then used for the glutathione-mediated intracellular delivery of the anticancer drug doxorubicin (DOX) into tumor cells. The polymer could self-assemble into micelles with an average diameter of 135 nm in aqueous solution and load DOX at a total content of 3.6%. The hydrophilic PEG shell of these micelles could be shed in the presence of reducing agent dithiothreitol (DTT), which resulted in size change of the micelles. *In vitro* release studies revealed that DOX-loaded mPEG-S-S-$(PCL)_2$ micelles exhibited faster DOX release in the presence of DTT. MTT assay demonstrated that DOX-loaded mPEG-S-S-$(PCL)_2$ micelles showed higher cytotoxicity against 10 mM of glutathione monoester (GSH-OEt) pretreated HeLa cells than that of the non-pretreated ones. Confocal laser scanning microscopy and flow cytometry analyses indicated that DOX-loaded mPEG-S-S-$(PCL)_2$ micelles were efficiently internalized into HeLa cells and exhibited faster DOX release in GSH-OEt-pretreated cells than in cells with no pretreatment. Endocytosis inhibition results proved that mPEG-S-S-$(PCL)_2$ micelles entered the cells mainly through the clathrin-mediated endocytosis pathway, and caveolae-mediated endocytosis was involved to a small extent. These results indicate the great potential of the proposed Y-shaped reduction-sensitive polymer for application in effective intracellular anticancer drug delivery.

1. Introduction

Anticancer drug delivery system aims to design carriers that can specifically and rapidly release encapsulated anticancer drugs inside tumor cells at increased concentrations but with reduced toxic side effects to enhance therapeutic efficacy [1–3]. Various nanoparticles (NPs), such as polymeric micelles [4], liposomes [5], inorganic NPs [6], and hybrid NPs [7], have been developed as carriers for intracellular drug release. Among these NPs, self-assembled polymeric micelles are the most promising nanocarrier system because of their largely enhanced drug solubility in water, prolonged blood circulation time, enhanced permeability and retention (EPR) effect for passive tumor targeting, improved drug bioavailability, and reduced systemic side effects [8–11]. However, the concentration of anticancer drugs in the intracellular compartments of cancer cells is often insufficient for killing cancer cells because of the low dose of the anticancer drug released or the slow release of the drug from polymeric micelles [12]. Therefore, the development of polymeric micellar delivery systems with rapid drug release rates after micelles arrival at the target site is urgently necessary to enhance chemotherapeutic efficacy and reduce drug resistance in cancer cells.

Stimuli-triggered shell-sheddable micelles that can shed their shells in response to minute environmental changes have been explored for drug delivery to protect the drug during circulation *in vivo* and enhance drug effects by releasing it specifically and rapidly into the cellular compartments [13,14]. A variety of stimuli triggers have been studied, including pH, redox potential, and various enzymes [15–18]. Reduction-triggered shell-sheddable polymeric micelles have been extensively studied for rapid drug release because of the existence of a high difference in redox potential between the mildly oxidizing extracellular milieu and the reducing intracellular fluids [19,20]. Moreover, tumor tissues are highly reducing and more hypoxic than normal tissues, with

* Corresponding author. Tel.: +86 27 68755317; fax: +86 27 68755317.
E-mail address: swhuang@whu.edu.cn (S.-W. Huang).

http://dx.doi.org/10.1016/j.colsurfb.2015.03.040
0927-7765/

at least fourfold higher concentrations of reducing agents in tumor tissues [21,22]. Reduction-triggered shell-sheddable micelles usually contain disulfide linkages between their hydrophilic shell and hydrophobic core. Disulfide bonds are stable under normal physiological conditions but reversibly cleavable in response to reductive conditions [23]. Reduction-triggered shell-sheddable micelles are designed to release encapsulated drugs quickly by shedding off their hydrophilic shell caused by disulfide bond cleavage under the reductive environment of intracellular fluids in cancer cells. Various reduction-triggered shell-sheddable micelles for intracellular drug delivery systems that allow rapid drug release inside cells and enhanced drug efficacy have recently been investigated [24–26].

Self-assembled polymeric micelles based on traditional amphiphilic linear block copolymers are one of the most investigated micellar systems for the controlled release of various anticancer drugs [27]. However, micelles formed from linear amphiphilic copolymers suffer from low encapsulation efficiency and high initial release rates [28]. Researches found that the presence of a branching point in polymer can reduce the conformational entropy and lead to self-assembled nanostructures different from those observed from their linear counterparts, improving several aspects of drug delivery, including drug loading efficiency, drug release rate, *in vivo* circulation, and biodistribution [29]. Poly(ethylene glycol) (PEG), the most popular hydrophilic block among the amphiphilic polymers, is nontoxic, biodegradable, and biocompatible. Micelles formed with a PEG-based shell show reduced uptake by macrophages of the mononuclear phagocyte system and provide relatively long plasma residence times [30]. Poly(ε-caprolactone) (PCL) is aliphatic polyester, which is widely applied in medical devices and is approved use by US food and Drug Administration (FDA) [31]. Several studies have shown that branching PCLs have distinct properties, such as lower solution viscosity and smaller hydrodynamic radius than that of the linear ones with the same composition and molecular weight. In addition, micelles formed from branching PCLs have lower critical micelle concentrations (CMCs), reduced crystallinity of the hydrophobic core and higher stability [32].

This study developed a new type of shell-sheddable micelles for reduction-triggered intracellular doxorubicine (DOX) delivery based on a Y-shaped amphiphilic polymer mPEG-S-S-$(PCL)_2$ with disulfide linkages between the hydrophobic polyester core and hydrophilic PEG shell. The resulting amphiphilic polymer could self-assemble in aqueous conditions to form micelles and encapsulate the anticancer drug DOX with excellent loading capability. The effective shedding of PEG shells in the presence of the reducing agent DTT, was monitored by dynamic light scattering (DLS) measurements. The rapid release of DOX under a reducing stimulus was demonstrated by *in vitro* release studies. The *in vitro* cytotoxicity of the DOX-loaded micelles was determined by MTT assay using human cervical cancer (HeLa) cells in the presence or absence of glutathione monoester (GSH-OEt). The intracellular release behavior of DOX was demonstrated with GSH-OEt-pretreated HeLa cells or non-pretreated ones by confocal laser scanning microscopy (CLSM) and flow cytometry (FCM). Finally, investigations on the internalization pathways of the micelles in HeLa cells with three different types of endocytosis inhibitors were investigated by CLSM and FCM. The results indicate the great potential of Y-shaped reduction-sensitive amphiphilic polymers for application in effective intracellular anticancer drug delivery systems.

2. Materials and methods

2.1. Materials

Synthesis of the polymer mPEG-S-S-$(PCL)_2$ was described in details in the Supplementary information. Monocarboxy-ω-monomethoxy PEG (mPEG-COOH; Mn = 5000 Da) and mono-BOC-cystamine were synthesized according to the method described previously [33,34]. Doxorubicin hydrochloride (DOX·HCl; Shanghai Yingxuan Co.) and dithiothreitol (DTT; >98%, Merck) were used as received.

2.2. Reduction-triggered disassembly of micelles

The size change of mPEG-S-S-$(PCL)_2$ micelles in response to 10 mM DTT in phosphate-buffered saline (PBS; 10 mM, pH 7.4) was monitored by DLS. Briefly, 10 mM DTT was added to a glass cell containing 1.0 mL of micellar solution in PBS. The solution was placed in a shaking bed at 37 °C and a rotation speed of 120 rpm. The micelle size was measured by DLS at different time intervals. The size of particles in a micellar solution in PBS without DTT was also measured as a control.

2.3. Preparation of DOX-loaded micelles

DOX-loaded polymeric micelles were prepared as follows: DOX·HCl (5 mg) was stirred overnight with twice the number of moles of TEA in 10 mL of DMSO to obtain the DOX base. After addition of mPEG-S-S-$(PCL)_2$ polymer (50 mg), the solution was stirred at room temperature for another 2 h. The final mixture was slowly added into 5 mL of ultrapure water with stirring, transferred to a dialysis tube, and dialyzed against ultrapure water at 25 °C for 24 h. Water was exchanged three times every 4 h for the first 12 h and then twice during the following 12 h. The solution in the dialysis tube was then filtered through a syringe filter (pore size = 0.45 μm) to remove the unloaded DOX. The entire procedure was performed in the dark.

The DOX concentration in DMSO was determined by fluorescence measurement using a calibration curve constructed from DOX/DMSO solutions with different DOX concentrations. The drug loading content (DLC) was calculated according to the following formula:

$$\mathrm{DLC\,(wt\%)} = \left(\frac{\text{weight of loaded drug}}{\text{weight of drug-loaded micelles}}\right) \times 100\%$$

2.4. In vitro *reduction-triggered DOX release*

Briefly, the DOX-loaded micelles of mPEG-S-S-$(PCL)_2$ were diluted to 1 mg/mL, and then 0.5 mL of this solution was transferred to a membrane tubing. It was immersed into a tube containing 10 mL of PBS (10 mM, pH 7.4) or PBS with 10 mM DTT in a shaking water bath at 37 °C to acquire sink conditions. At predetermined time intervals, 5 mL of the external buffer was withdrawn and replaced with 5 mL of fresh corresponding buffer solution. The amount of DOX released was determined by fluorescence measurements at 485 nm excitation. The experiments were conducted in triplicate and the results are expressed as averaged data with standard deviations.

2.5. In vitro *cytotoxicity assay*

The cytotoxicity of mPEG-S-S-$(PCL)_2$ micelles, DOX-loaded mPEG-S-S-$(PCL)_2$ micelles, and free DOX against HeLa cells were evaluated *in vitro* by MTT assay. Briefly, HeLa cells were seeded into a 96-well plate at a density of 5.0×10^3 cells/well in 100 μL of complete DMEM containing 10% FBS and cultured for 1 d at 37 °C in a 5% CO_2 atmosphere. The cells were then incubated with mPEG-S-S-$(PCL)_2$ micelles, DOX-loaded mPEG-S-S-$(PCL)_2$ micelles, or free DOX for 48 h at 37 °C. The concentrations of mPEG-S-S-$(PCL)_2$ micelles ranged from 3.7 mg/L to 500 mg/L. DOX-loaded mPEG-S-S-$(PCL)_2$ micelles or free DOX were diluted in complete DMEM with final DOX concentrations ranging from 0.08 μg/mL to 10 μg/mL.

MTT stock solution (5 mg/mL in PBS, 20 μL) was added to each well and the cells were incubated for another 4 h. After complete removal of the medium, 150 μL of DMSO was added to each well to dissolve the formazan blue crystals. The absorbance of the solution was measured using a microplate reader at 570 nm. Cell viability was expressed as follows: Cell viability (%) = $A_{sample}/A_{control} \times 100\%$, where A_{sample} and $A_{control}$ are the absorbance values of the treated cells and untreated control cells, respectively. A_{sample} and $A_{control}$ values were obtained after subtracting the absorbance of DMSO. Data are presented as average ± standard deviation ($n = 4$).

We further investigated the influence of GSH-OEt on the cytotoxicity of DOX-loaded mPEG-S-S-$(PCL)_2$ micelles. Briefly, cells were cultured for 1 d at 37 °C in a 5% CO_2 atmosphere and treated with 10 mM GSH-OEt for 2 h. Cells without pretreatment were used as controls. Cells were washed with PBS to remove the GSH-OEt and then DOX-loaded mPEG-S-S-$(PCL)_2$ micelles diluted in complete DMEM (200 μL) with the DOX concentration of 1 μg/mL or 2 μg/mL were added to cells and further incubated for 48 h. MTT stock solution (5 mg/mL in PBS, 20 μL) was added to each well, and the cells were incubated for another 4 h. After complete removal of the medium, 150 μL of DMSO was added to each well to dissolve the formazan blue crystals. Cell viability (%) was determined by the same method described above.

2.6. Cellular uptake of DOX-loaded micelles

Intracellular DOX release from DOX-loaded mPEG-S-S-$(PCL)_2$ micelles was monitored by CLSM and FCM.

CLSM was employed to observe the intracellular distribution of DOX. Briefly, HeLa cells were seeded into a confocal dish at a density of 1.5×10^5 cells/well in 1.5 mL of complete DMEM containing 10% FBS and cultured for 1 d at 37 °C in a 5% CO_2 atmosphere prior to treatment with GSH-OEt for 2 h. Cells without pretreatment were used as the control. After GSH-OEt was washed off with PBS, DOX-loaded mPEG-S-S-$(PCL)_2$ micelles in DMEM at a final DOX concentration of 2 μg/mL were added to cells and incubated for 4 or 24 h at 37 °C. After each time point, the culture medium was removed and the dish was washed with PBS three times for 1 min each to remove DOX-loaded micelles that had not been ingested by the cells. Thereafter, the cells were fixed with 4% (w/v) paraformaldehyde aqueous solution for 10 min at room temperature, and the dish was washed with PBS three times for 5 min each. Finally, the cells were stained with Hoechst 33258 (5 μg/mL in PBS) at 37 °C for 8 min, and the dish was washed with PBS three times for 5 min each. The obtained confocal dish was examined by CLSM (Nikon, TE2000, EZ-C1, Japan).

FCM was used to further investigate the uptake of DOX-loaded mPEG-S-S-$(PCL)_2$ micelles against HeLa cells. Briefly, HeLa cells were seeded into a 6-well plate at a density of 4.0×10^5 cells/well in 4 mL of complete DMEM containing 10% FBS and cultured for 24 h at 37 °C in a 5% CO_2 atmosphere prior to treatment with GSH-OEt for 2 h. Cells without pretreatment were used as controls. After the GSH-OEt had been washed off with PBS, DOX-loaded mPEG-S-S-$(PCL)_2$ micelles in DMEM at a final DOX concentration of 2 μg/mL were added to cells and incubated for 4 or 24 h at 37 °C. After each time point, the culture medium was removed, and the cells were washed twice with PBS to remove DOX-loaded micelles that had not been ingested by the cells, detached with trypsin for 1 min, and then terminated by complete DMEM containing 10% FBS. Approximately 8 mL of PBS was added to each well, and the cell suspensions were centrifuged at 1000 rpm for 5 min. After removal of the supernatant, the cells were resuspended in 8 mL of PBS and centrifuged again. The cells were resuspended in 500 μL of PBS and filtered through a 40 μm nylon mesh to remove cell aggregates before measurements were made. The mean fluorescence intensity (MFI) of DOX in cells was analyzed using flow cytometry (Epics XL) at an excitation wavelength of 488 nm.

2.7. Endocytosis pathway of DOX-loaded micelles

We investigated the endocytosis pathway of DOX-loaded mPEG-S-S-$(PCL)_2$ micelles against HeLa cells using FCM and CLSM.

FCM HeLa cells were seeded into 6-well plates at a density of 4.0×10^5 cells/well in 4 mL of complete DMEM containing 10% FBS and cultured for 1 d at 37 °C in a 5% CO_2 atmosphere. To determine the effect of various inhibitors on micelles uptake, the cells were separately pre-incubated for 30 min with three different endocytosis inhibitors at concentrations considered not toxic to the cells (5 mM methyl-β-cyclodextrin (MBCD), 0.45 M sucrose, or 5 μM cytochalasin D) [35]. After removal of the inhibitor solutions, freshly prepared DOX-loaded mPEG-S-S-$(PCL)_2$ micelles (DOX concentration: 2 μg/mL) in DMEM containing inhibitors at the same concentrations above were added and further incubated for 2 h. The subsequent steps were similar to those described in Section 2.6 – FCM. The group without any treatment was used as a background during FCM analysis.

CLSM HeLa cells were seeded into a confocal dish at a density of 1.5×10^5 cells/well in 1.5 mL of complete DMEM containing 10% FBS and cultured for 1 d at 37 °C in a 5% CO_2 atmosphere. The cells were separately pretreated for 30 min with three different endocytosis inhibitors at concentrations considered not toxic to the cells (5 mM MBCD, 0.45 M sucrose, or 5 μM cytochalasin D). After removal of the inhibitor solutions, the freshly prepared DOX-loaded mPEG-S-S-$(PCL)_2$ micelles (DOX concentration: 2 μg/mL) in DMEM containing inhibitors at the same concentrations above were added and further incubated for 2 h. The subsequent steps are similar to those described in Section 2.6 – CLSM. A group with the test materials but without inhibitor treatment was used as the control.

3. Results and discussion

3.1. Synthesis of Y-shaped amphiphilic polymer mPEG-S-S-$(PCL)_2$

The synthesis procedure of Y-shaped amphiphilic polymer mPEG-S-S-$(PCL)_2$ is illustrated in Fig. S1. mPEG-S-S-$(PCL)_2$ was prepared by ring-opening polymerization of ε-CL initiated by terminal hydroxyl groups of mPEG-S-S-$(OH)_2$ using $Sn(Oct)_2$ as the catalyst. Synthesis of the macroinitiator mPEG-S-S-$(OH)_2$ included three steps as follows: First, mPEG-S-S-NH_2 was obtained by a condensation reaction between mPEG-COOH and mono-BOC-cystamine. Then, the obtained product mPEG-S-S-NH-BOC was unprotected with TFA. mPEG-COOH and mono-BOC-cystamine were synthesized according to a procedure described previously. Second, mPEG-S-S-$(OCH_3)_2$ was prepared by Michael addition of the primary amine and di-secondary amine of mPEG-S-S-NH_2 with methyl acrylate by to introduce a branching point to the polymer. Finally the macroinitiator mPEG-S-S-$(OH)_2$ was synthesized by transesterification between mPEG-S-S-$(OCH_3)_2$ and excess ethanolamine. Hydroxyl groups were introduced on the end of the polymer, which initiated the ring-opening polymerization of ε-caprolactone.

The structures of mPEG-COOH, mono-BOC-cystamine, mPEG-S-S-NH_2, and mPEG-S-S-$(PCL)_2$ were confirmed using ^1H NMR. As shown in Fig. S2A, peaks appeared at δ 4.165 and 3.878 ppm were observed, indicating the successful synthesis of mPEG-COOH. Fig. S2B shows the ^1H NMR spectrum of mono-BOC-cystamine. Signals assigned to both cystamine (δ 4.949, 3.460, 3.012, 2.793, and 1.399 ppm) and di-tert-butyl dicarbonate (δ 1.449) were observed in the spectrum. Comparison of the integrals of signals at δ 2.793

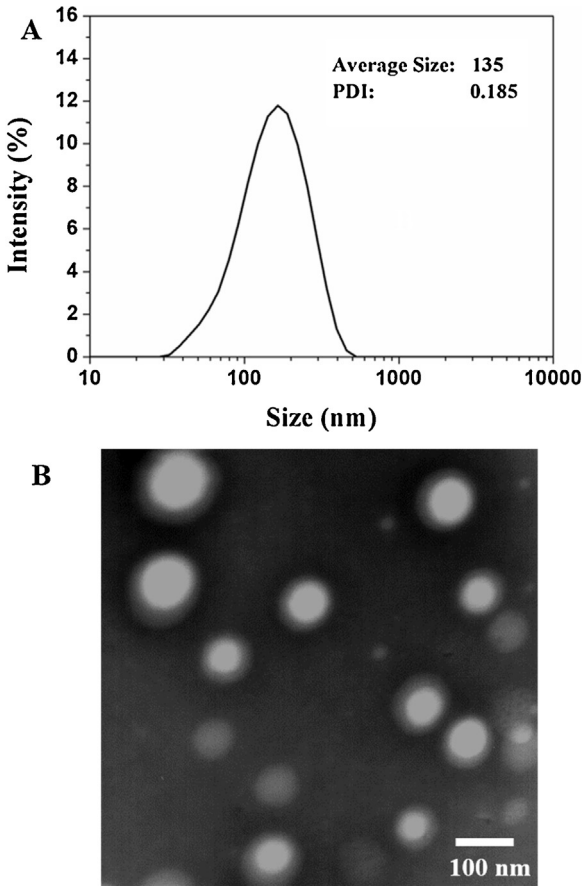

Fig. 1. Size distribution of mPEG-S-S-$(PCL)_2$ micelles as determined by (A) DLS and (B) TEM.

and 1.449 ppm showed equivalent coupling of cystamine and di-tert-butyl dicarbonate. The ^{1}H NMR spectrum of mPEG-S-S-NH_2 is shown in Fig. S2C. Signals assigned to both mPEG (δ 4.001, 3.881, 3.648, and 3.426 ppm) and cystamine (δ 3.408, 3.065, and 2.957 ppm) were observed in the spectrum. The signal assigned to mPEG-COOH (δ 4.165) disappeared, and a peak attributed to methylene protons neighboring the amido bond (—CH_2—CO—NH—) (δ 4.001 ppm) was detected. As shown in Fig. S2D, the peak at δ 3.693 ppm was attributed to the mPEG block. The peaks at δ 4.106, 2.357, 1.696, and 1.424 ppm were assigned to PCL block. The mass ratio of the mPEG block to the PCL block was found to be 5000:4235 calculated based on the integrated intensity of signals at δ 3.693 ppm from mPEG and at δ 4.106 from PCL. These results support the successful synthesis of the Y-shaped amphiphilic polymer mPEG-S-S-$(PCL)_2$.

3.2. Preparation and characterization of micelles

Amphiphilic copolymers tend to form core–shell structural micelles in selective solvents. In this study, micelles of mPEG-S-S-$(PCL)_2$ were prepared by dialysis method. The micellar structure was confirmed by DLS and TEM. DLS results showed that mPEG-S-S-$(PCL)_2$ formed micelles with an average size of ~135 nm and a narrow size distribution (PDI = 0.185; Fig. 1A). TEM micrographs confirmed that mPEG-S-S-$(PCL)_2$ micelles have a spherical morphology with an average size of approximately 90 nm (Fig. 1B). The mean diameters of micelles determined by TEM were less than the values measured by DLS likely because the diameter obtained from DLS reflects the hydrodynamic diameter of the micelles whereas the diameter observed by TEM indicates that of dried micelles. The

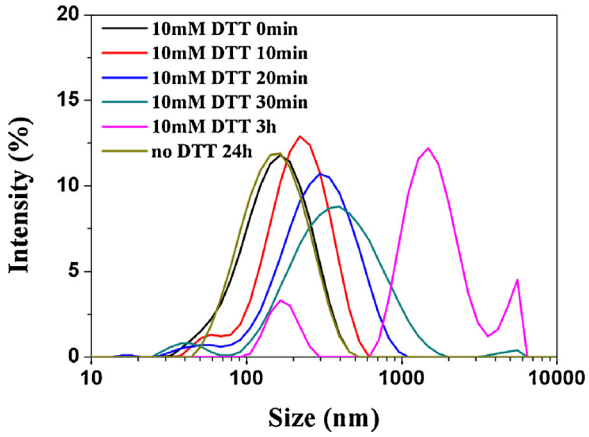

Fig. 2. Size change of mPEG-S-S-$(PCL)_2$ micelles in response to 10 mM DTT in PBS (10 mM, pH 7.4) as determined by DLS.

CMC was determined using pyrene as a spectroscopic probe. mPEG-S-S-$(PCL)_2$ showed a low CMC of 15.6 mg/L, which may provide the possibility of keeping stabilization of micelles and allowing their use in very dilute aqueous milieu such as blood and body fluids.

3.3. Reduction-triggered disassembly of micelles

Disulfide linkages can be readily reduced into free thiols in the presence of reducing agents. We expected that mPEG-S-S-$(PCL)_2$ micelles will reductively shed their PEG shells in response to DTT. To demonstrate this responsiveness, the size change of micelles in response to 10 mM DTT in PBS was determined by DLS measurements. Fig. 2 shows that the average micelle size gradually increased within the first 30 min after addition of DTT. The micelle size increased from 135 nm to 304 nm in 30 min, indicating the detachment of hydrophilic PEG shells from the micelles and the enhanced hydrophobic interaction of the inner core. After 3 h, three populations at 164, 1484, and 5560 nm were clearly observed, demonstrating the complete destruction of the micelles, no nanoparticle was detected in the solution. However, no change in micelle size was observed even after 24 h in the absence of DTT under the same conditions.

3.4. DOX loading and reduction-triggered DOX release

Loading and *in vitro* drug release studies were performed to assess the feasibility of using mPEG-S-S-$(PCL)_2$ micelles as a reduction-sensitive anticancer drug delivery nanocarrier. In this study, DOX was used as a model anticancer drug. DOX is one of the most commonly used chemotherapeutic drugs and a popular research tool because of its inherent fluorescence. DOX have its cytotoxic effects through DNA intercalation, topoisomerase II inhibition, prevention of DNA and RNA synthesis, and the generation of reactive oxygen species [36].

DOX was loaded into micelles by dialysis of polymer/DOX solution of DMSO against ultrapure water. Prior to DOX loading into the micelles, DOX·HCl was stirred with twice the number of moles of TEA in DMSO to detach the HCl and render the drug hydrophobic. DLS measurement showed that the effect of DOX-loading on the micelle size was not obvious. The size of DOX-loaded mPEG-S-S-$(PCL)_2$ micelles was approximately 150 nm and the size distribution was 0.164. The micelle size is an important parameter for intracellular drug delivery. Small-sized micelles (<200 nm) are beneficial for the maintenance of low-level reticuloendothelial system uptake, minimal renal excretion, and effective EPR for passive tumor targeting [37]. The results indicated that the size of DOX-loaded

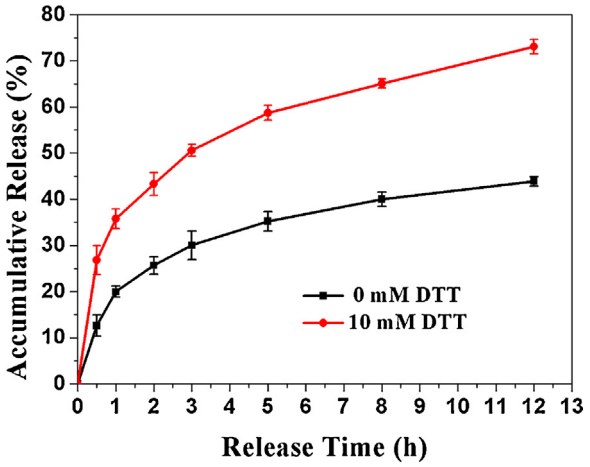

Fig. 3. Reduction-triggered release of DOX from DOX-loaded mPEG-S-S-$(PCL)_2$ micelles in PBS (10 mM, pH 7.4) with or without 10 mM DTT. The standard deviation for each data point was averaged over three samples ($n = 3$).

mPEG-S-S-$(PCL)_2$ micelles is suitable for intracellular drug delivery. The DLC was determined by fluorescence measurements. The theoretical DLC was set as 10 wt%, and the results showed that the calculated DLC of DOX-loaded mPEG-S-S-$(PCL)_2$ micelles was 3.6%.

Several studies have shown that the PEG shell may hinder drug release. To investigate the effect of PEG shell detachment on drug release from the DOX-loaded mPEG-S-S-$(PCL)_2$ micelles, we performed DOX release experiments with DOX-loaded mPEG-S-S-$(PCL)_2$ micelles in the presence or absence of 10 mM DTT. As shown in Fig. 3, a burst release was observed at the early stage of the profiles, which may be attributed to the presence of residual amounts of DOX on the micellar surfaces. In the presence of 10 mM DTT, a reductive environment analogous to that of the intracellular compartments such as cytosol and the cell nuclei, DOX-loaded mPEG-S-S-$(PCL)_2$ micelles showed a much faster DOX release rate, *i.e.*, 73% of the encapsulated DOX was released in 12 h. However, in the absence of DTT, less DOX was released, only 43% of loaded DOX was released. This result may be attributed to the cleavage of the disulfide bond in mPEG-S-S-$(PCL)_2$ micelles, which causes detachment of the PEG shell, destruction of the micelles, and accelerated release of encapsulated DOX. These results suggest that reduction-sensitive micelles may achieve site-specific drug delivery in the presence of reducing agents.

3.5. MTT assay

HeLa cells were co-cultured with mPEG-S-S-$(PCL)_2$ micelles at different concentrations. As shown in Fig. S3, compared with the blank control, HeLa cells were not influenced by the addition of micelles. The mPEG-S-S-$(PCL)_2$ micelles featured innocuity at concentrations from 3.7 mg/L to 500 mg/L on HeLa cells.

The cytotoxicity of DOX-loaded mPEG-S-S-$(PCL)_2$ micelles and free DOX against HeLa cells was determined by MTT assay. As shown in Fig. 4A, the IC_{50} of DOX-loaded mPEG-S-S-$(PCL)_2$ micelles and free DOX were determined as ~0.4, and ~2.6 μg/mL, respectively. Compared with free DOX, the DOX-loaded micelles exhibited lower cytotoxicity to HeLa cells at the same DOX dosage. As DOX is a small molecule, it can be rapidly transported into cells by passive diffusion. By contrast, DOX-loaded micelles are internalized only by endocytosis and the progressive release of encapsulated DOX may delay drug delivery.

Further cytotoxicity studies were conducted to investigate whether or not PEG shell detachment of the DOX-loaded mPEG-S-S-$(PCL)_2$ micelles affects HeLa cell proliferation. Briefly, DOX-loaded mPEG-S-S-$(PCL)_2$ micelles were incubated with HeLa cells that had either been non-pretreated or pretreated with 10 mM GSH-OEt for 2 h; the final DOX concentration was either 1 or 2 μg/mL. Fig. 4B shows significant differences in cytotoxicity between GSH-OEt-pretreated and non-pretreated cells. Incubation of DOX-loaded mPEG-S-S-$(PCL)_2$ micelles with GSH-OEt-pretreated HeLa cells showed significantly higher cytotoxicity than non-pretreated cells at both DOX concentrations. Previous studies have indicated that GSH-OEt can generate high intracellular concentrations of GSH by ethyl ester hydrolyzation in the cytoplasm [38]. The results may be attributed to the rapid release of DOX from DOX-loaded mPEG-S-S-$(PCL)_2$ micelles by shedding of the PEG shell in an intracellular compartment with high GSH concentrations, which enhance its drug effect.

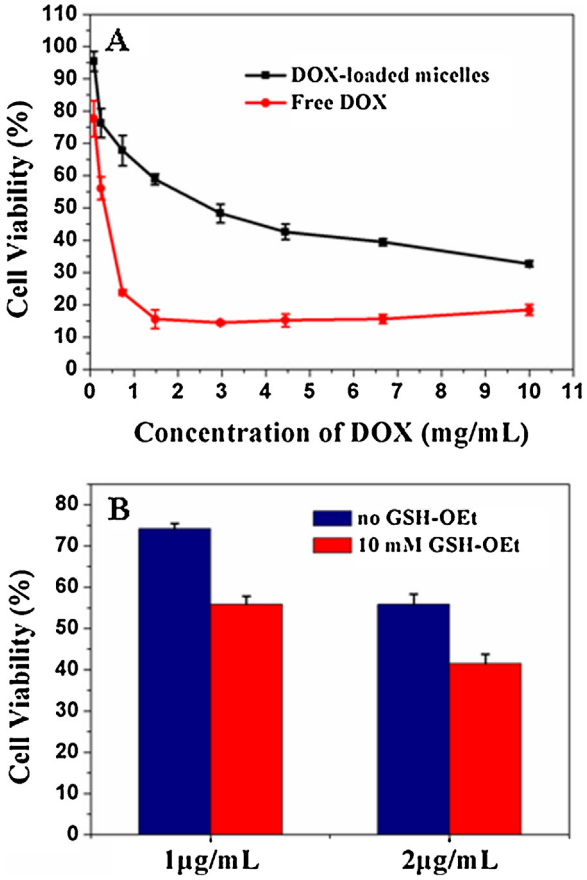

Fig. 4. Cytotoxicity studies of (A) DOX-loaded mPEG-S-S-$(PCL)_2$ micelles or free DOX in HeLa cells after incubation for 48 h and (B) DOX-loaded mPEG-S-S-$(PCL)_2$ micelles incubated with GSH-OEt pretreated or non-pretreated HeLa cells after 48 h. The standard deviation of each data point was averaged from four samples ($n = 4$).

3.6. Intracellular DOX release

GSH-OEt can generate high intracellular concentrations of GSH by ethyl ester hydrolyzation in the cytoplasm. In this study, we investigated the cellular uptake of mPEG-S-S-$(PCL)_2$ micelles against HeLa cells using CLSM and FCM to determine whether or not these micelles function in a high-intracellular GSH environment.

As a model system, Hela cells were incubated with GSH-OEt for 2 h to increase intracellular concentrations of GSH. HeLa cells without GSH-OEt pretreatment were used as controls. After incubation of DOX-loaded mPEG-S-S-$(PCL)_2$ micelles with pretreated or non-pretreated HeLa cells for 4 or 24 h, the cells were observed by CLSM. As shown in Fig. 5A and B, DOX fluorescence could be detected inside the cells after only 4 h incubation with DOX-loaded mPEG-S-S-$(PCL)_2$ micelles, indicating the rapid internalization of

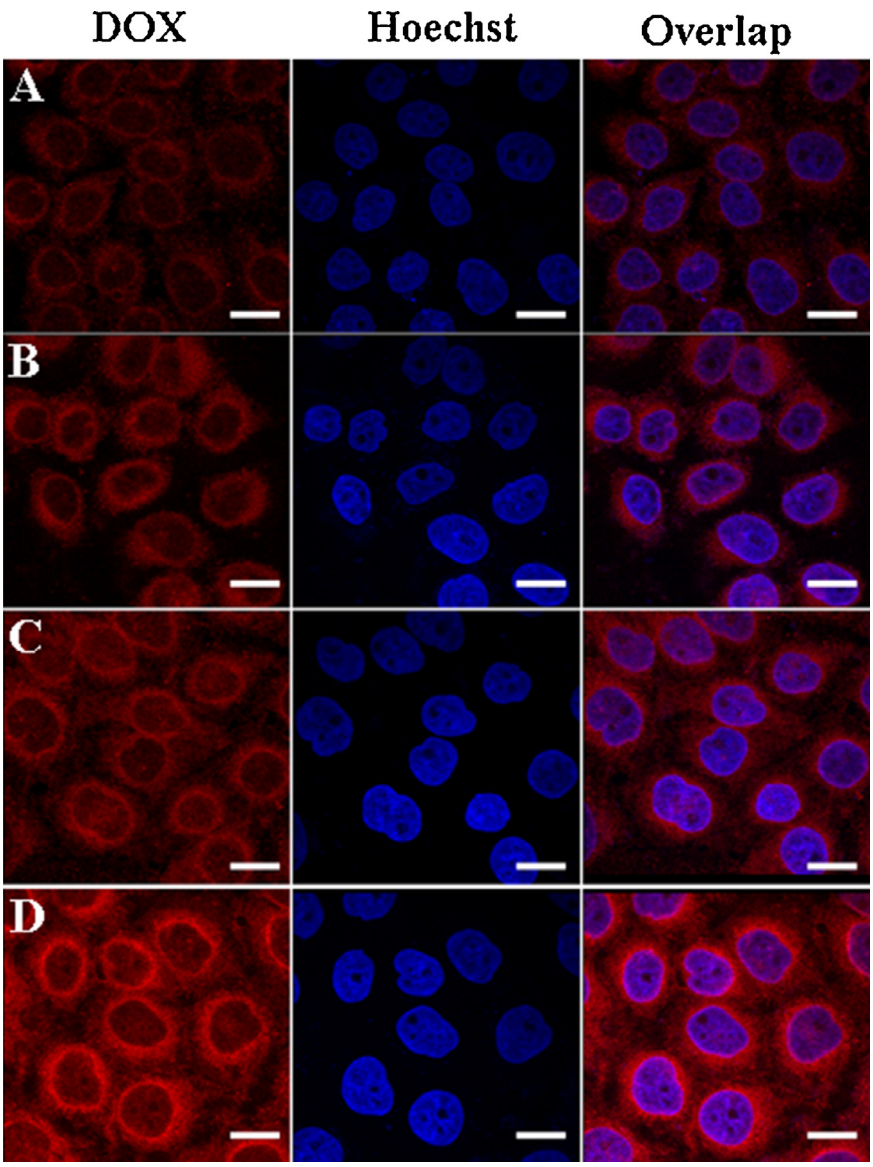

Fig. 5. CLSM images of non-pretreated HeLa cells after (A) 4 h and (C) 24 h incubation and GSH-OEt-pretreated HeLa cells after (B) 4 h and (D) 24 h incubation with DOX-loaded mPEG-S-S-$(PCL)_2$ micelles. DOX dosage was 2 μg/mL. Scale bar is 20 μm.

micelles and release of DOX inside the cells. GSH-OEt pretreated Cells incubated with the DOX-loaded mPEG-S-S-$(PCL)_2$ micelles emitted stronger DOX fluorescence compared with the non-pretreated cells. The intensity of the DOX fluorescence inside the cells was further increased by prolonging the incubation time to 24 h. Fig. 5C and D shows that the difference in DOX fluorescence intensity between pretreated cells and non-pretreated cells was highly significant; much stronger DOX fluorescence was observed

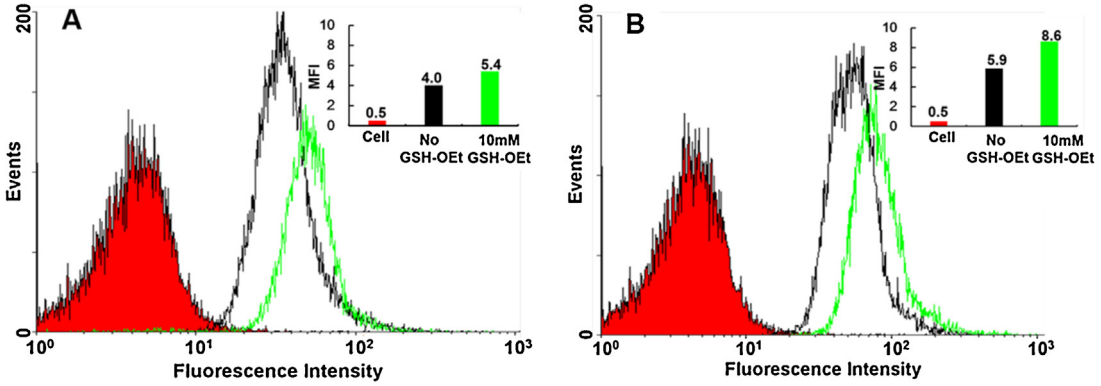

Fig. 6. FCM analyses of HeLa cells with or without GSH-OEt pretreatment after (A) 4 h and (B) 24 h incubation with DOX-loaded mPEG-S-S-$(PCL)_2$ micelles. DOX dosage was 2 μg/mL.

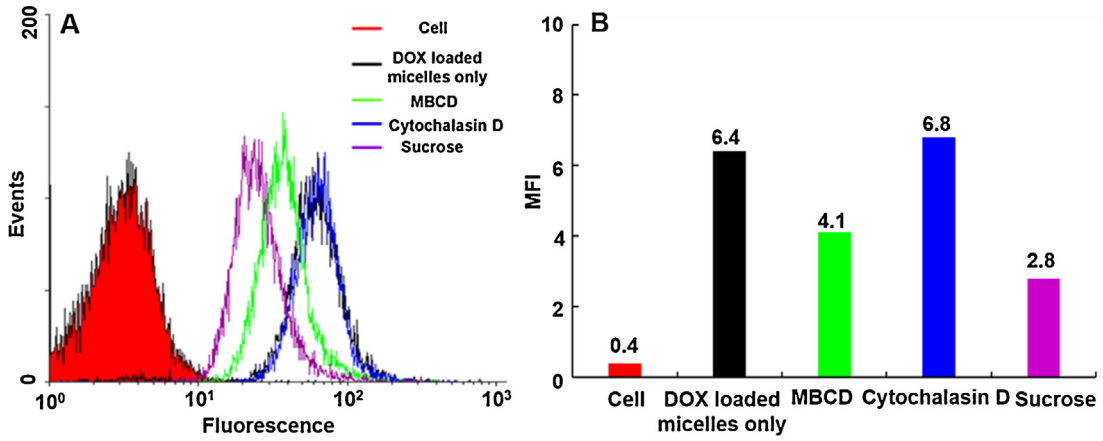

Fig. 7. Effect of endocytosis inhibitors on the cellular uptake of DOX-loaded mPEG-S-S-$(PCL)_2$ micelles as determined by FCM analysis. DOX dosage was 2 μg/mL.

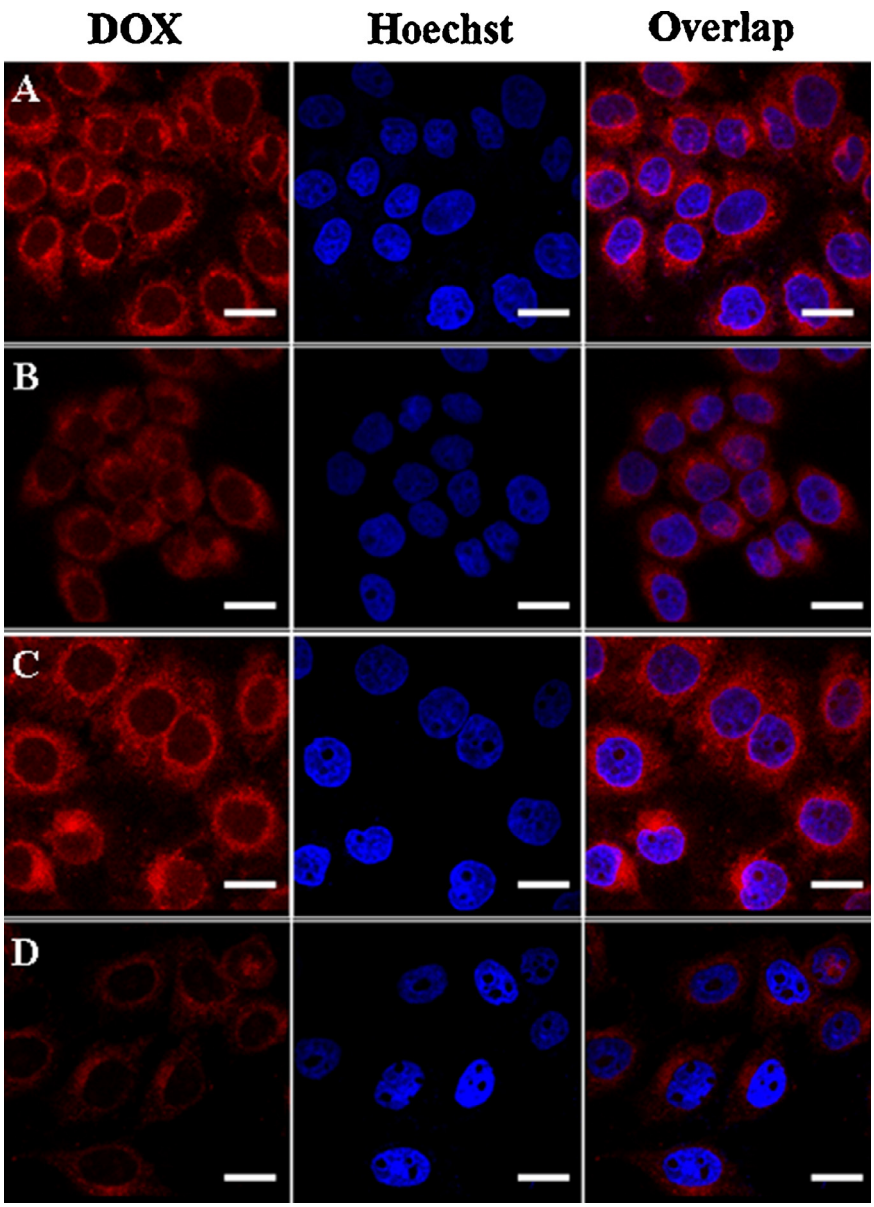

Fig. 8. CLSM images of HeLa cells after incubation with DOX-loaded mPEG-S-S-$(PCL)_2$ micelles containing different endocytosis inhibitors: (A) none, (B) MBCD, (C) cytochalasin D, and (D) sucrose. DOX dosage was 2 μg/mL. Scale bar is 20 μm.

in the nuclei and cytoplasm of GSH-OEt-pretreated cells than in non-pretreated ones. DOX fluorescence is observed only when DOX is released into cells because of the self-quenching effect of DOX in NPs [39]. These images confirm that destabilization of mPEG-S-S-$(PCL)_2$ micelles by high intracellular GSH concentrations accelerates the release of DOX and promotes its subsequent accumulation in cell nuclei. Disulfide bonds are rapidly cleaved in response to variations in intracellular levels of reducing potential, causing DOX to burst-release from disrupted micelles and readily diffuse into the cell nuclei. These results are consistent with findings from the cytotoxicity studies. DOX-loaded mPEG-S-S-$(PCL)_2$ micelles showed higher cytotoxicity to GSH-OEt-pretreated cells than non-pretreated ones. This effect may be attributed to the rapid release of DOX in GSH-OEt-pretreated cells.

The intracellular drug release against HeLa cells incubated with DOX-loaded mPEG-S-S-$(PCL)_2$ micelles was further studied by FCM. HeLa cells were pretreated with 10 mM of GSH-OEt and then incubated with DOX-loaded mPEG-S-S-$(PCL)_2$ micelles for 4 or 24 h. HeLa cells without GSH-OEt pretreatment were measured as controls. FCM analysis results were consistent with the CLSM findings. Fig. 6 shows the mean DOX fluorescence intensity in HeLa cells after incubation with DOX-loaded mPEG-S-S-$(PCL)_2$ micelles for 4 or 24 h. The MFI of the GSH-OEt-pretreated cells were higher than that of non-pretreated cells at both 4 and 24 h. Fluorescence signals are associated with the quantity of DOX released from the micelles. Enhanced intracellular DOX fluorescence in GSH-OEt-pretreated cells indicates rapid and complete intracellular DOX release in the presence of high GSH concentrations. These results are identical to the CLSM and *in vitro* cytotoxicity findings.

3.7. Endocytosis pathway

We studied the internalization pathway of DOX-loaded mPEG-S-S-$(PCL)_2$ micelles using three different types of endocytosis inhibitors. An in-depth understanding of polymeric micelle–cell interactions will enable the development of better drug delivery systems for cancer therapy. Micelles are always internalized by cells through endocytosis because of their relatively large size. Endocytosis can be divided into two broad categories: phagocytosis and pinocytosis. Pinocytosis can be further divided into macropinocytosis, clathrin-mediated endocytosis, and caveolae-mediated endocytosis. This study used three different types of inhibitors as follows: MBCD for caveolae-mediated endocytosis, hypertonic sucrose for clathrin-mediated endocytosis, and cytochalasin D for macropinocytosis.

Fig. 7 shows the mean DOX fluorescence intensity in HeLa cells after incubation with DOX-loaded mPEG-S-S-$(PCL)_2$ micelles with or without endocytosis inhibitors for 2 h. The entry of mPEG-S-S-$(PCL)_2$ micelles into the cells was blocked in the presence of MBCD and hypertonic sucrose but unaffected by cytochalasin D. These findings suggest that micelles enter cells *via* caveolae- and clathrin-mediated endocytosis. Although MBCD had some effect on micellar uptake, its effect was much less pronounced than that of hypertonic sucrose. The greatest inhibition of micelles entry into HeLa cells was observed with hypertonic sucrose, which indicates that the most prominent pathway for micelles uptake is clathrin-mediated endocytosis.

The CLSM results were consistent with the FCM findings. Fig. 8 shows that the DOX fluorescence of cells treated with MBCD and hypertonic sucrose was weaker than that of cells incubated with DOX-loaded mPEG-S-S-$(PCL)_2$ micelles only, especially in cells cultured with hypertonic sucrose. The DOX fluorescence intensity of cells in the presence of cytochalasin D was similar to that in cells treated with DOX-loaded mPEG-S-S-$(PCL)_2$ micelles only. This result indicates that DOX-loaded micelles enter cells through both caveolae- and clathrin-mediated endocytosis; of these, the most prominent pathway is clathrin-mediated endocytosis, which is recognized as the fastest and most highly regulated pathway for the internalization of nanocarriers and macromolecules.

4. Conclusion

A novel Y-shaped amphiphilic polymer mPEG-S-S-$(PCL)_2$ was synthesized for the intracellular delivery of DOX. The polymer was self-assembled into micellar aggregates in aqueous solution and loaded with DOX at high DLC. *In vitro* release studies revealed that DOX-loaded mPEG-S-S-$(PCL)_2$ micelles released DOX rapidly in the presence of DTT. Cell experiments showed that DOX-loaded mPEG-S-S-$(PCL)_2$ micelles efficiently delivered DOX to the cell nuclei and displayed higher cytotoxicity against GSH-OEt-pretreated HeLa cells than non-pretreated cells. Endocytosis inhibition results indicated that the DOX-loaded mPEG-S-S-$(PCL)_2$ micelles entered cells mainly through the clathrin-mediated endocytosis pathway, which is recognized as the fastest and most highly regulated pathway for the internalization of nanocarriers and macromolecules. Reduction-sensitive micelles based on the novel Y-shaped amphiphilic polymer mPEG-S-S-$(PCL)_2$ are promising carriers for reduction-sensitive anticancer drug delivery systems.

Acknowledgements

This work was financially supported by National Natural Science Foundation of China (51473127, 51273150) and National Basic Research Program of China (2011CB606202).

Appendix A. Supplementary data

Supplementary data associated with this article can be found, in the online version, at http://dx.doi.org/10.1016/j.colsurfb.2015.03.040.

References

[1] H.M. Liu, C.M. Qiao, J. Yang, J. Weng, X. Zhang, J. Mater. Chem. B 35 (2014) 5910.
[2] M. Gupta, G.P. Agrawal, S.P. Vyas, Curr. Mol. Med. 13 (2013) 179.
[3] N. Graf, S.J. Lippard, Adv. Drug Deliv. Rev. 64 (2012) 993.
[4] Z. Ahmad, A. Shah, M. Siddig, H.B. Kraatz, RSC Adv. 4 (2014) 17028.
[5] J. Tang, H. Fu, Q.F. Kuang, L. Zhang, Q.Y. Zhang, Y.Y. Liu, R. Ran, H.L. Gao, Z.R. Zhang, Q. He, J. Drug Target. 4 (2014) 313.
[6] L.L. Li, F.Q. Tang, H.Y. Liu, T.L. Liu, N.J. Hao, D. Chen, X. Teng, J.Q. He, ACS Nano 4 (2010) 6874.
[7] W.T. Wu, J. Shen, Z. Gai, P. Banerjee, S.Q. Zhou, Biomaterials 32 (2011) 9876.
[8] S. Quader, H. Cabral, Y. Mochida, T. Ishii, X. Liu, K. Toh, H. Kinoh, Y. Miura, N. Nishiyama, K. Kataoka, J. Control. Release 188 (2014) 67.
[9] V.P. Torchilin, Pharm. Res. 24 (2007) 1.
[10] Y. Ohya, S. Takeda, Y. Shibata, T. Ouchi, A. Kano, T. Iwata, S. Mochizuki, Y. Taniwaki, A. Maruyama, J. Control. Release 155 (2011) 104.
[11] N.V. Cuong, Y.L. Li, M.F. Hsieh, J. Mater. Chem. 22 (2012) 1006.
[12] A. Lavasanifar, J. Samuel, G. Kwon, Adv. Drug Deliv. Rev. 54 (2002) 169.
[13] M. Nakayama, J. Akimoto, T. Okano, J. Drug Target. 7 (2014) 584.
[14] J. Liu, C. Detrembleur, A. Debuigne, M.C. De Pauw-Gillet, S. Mornet, L. Vancer Elst, S. Laurent, C. Labrugere, E. Duguet, C. Jerome, Nanoscale 23 (2013) 11464.
[15] L. Xing, Y.Y. Cao, S.A. Che, Chem. Commun. 48 (2012) 5995.
[16] H.Y. Wen, C.Y. Dong, H.Q. Dong, A.J. Shen, W.J. Xia, X.J. Cai, Y.Y. Song, X.Q. Li, Y.Y. Li, D.L. Shi, Small 8 (2012) 760.
[17] J.S. Mejia, E.R. Gillies, Polym. Chem. 6 (2013) 1969.
[18] M.A. Azagarsamy, P. Sokkalingam, S. Thayumanavan, J. Am. Chem. Soc. 131 (2009) 14184.
[19] P. Kuppusamy, M. Afeworki, R.A. Shankar, D. Coffin, M.C. Krishna, S.M. Hahn, Cancer Res. 58 (1998) 1562.
[20] B.K. Sourkohi, R. Schmidt, J.K. Oh, Macromol. Rapid Commun. 32 (2011) 1652.
[21] P. Kuppusamy, H. Li, G. Ilangovan, A.J. Cardounel, J.L. Zweier, K. Yamada, M.C. Krishna, J.B. Mitchell, Cancer Res. 62 (2002) 307.
[22] X.L. Zhang, K. Liu, Y.X. Huang, J.N. Xu, J. Li, X.C. Ma, S. Li, Bioconjug. Chem. 9 (2014) 1689.
[23] S.Y. Lee, S. Kim, J.Y. Tyler, K. Park, J.X. Cheng, Biomaterials 34 (2013) 552.
[24] W. Wang, H.L. Sun, F.H. Meng, S.B. Ma, H.Y. Liu, Z.Y. Zhong, Soft Matter 8 (2012) 3949.
[25] S.J. Yu, J.X. Ding, C.L. He, Y. Cao, W.G. Xu, X.S. Chen, Adv. Healthc. Mater. 5 (2014) 752.

[26] C. Cui, Y.N. Xue, M. Wu, Y. Zhang, P. Yu, L. Liu, R.X. Zhuo, S.W. Huang, Biomaterials 34 (2013) 3858.
[27] G.S. Kwon, M.L. Forrest, Drug Dev. Res. 67 (2006) 15.
[28] P.W. Dong, X.H. Wang, Y.C. Gu, Y.J. Wang, Y.J. Wang, C.Y. Gong, F. Luo, G. Guo, X. Zhao, Y.Q. Wei, Z.Y. Qian, Colloids Surf. A 358 (2010) 128.
[29] N. Hadjichristidis, H. Iatrou, M. Pitsikalis, S. Pispas, A. Avgeropoulos, Progr. Polym. Sci. 30 (2005) 725.
[30] K.R. Zhang, X. Tang, J. Zhang, W. Lu, X. Lin, Y. Zhang, B. Tian, H. Yang, H.B. He, J. Control. Release 183 (2014) 77.
[31] S.V. Lale, R.G. Aswathy, A. Aravind, D.S. Kumar, V. Koul, Biomacromolecules 5 (2014) 1737.
[32] W.J. Lin, S.Y. Nie, Q. Zhong, Y.Q. Yang, C.Z. Cai, J.F. Wang, L.J. Zhang, J. Mater. Chem. B 25 (2014) 4008.
[33] J. Xue, Z.F. Jia, X.L. Jiang, Y.P. Wang, L. Chen, L. Zhou, P. He, X.Y. Zhu, D.Y. Yan, Macromolecules 39 (2006) 8905.
[34] H. Niu, Z.H. Liu, L. Fu, F. Shi, H.W. Ma, Y. Ozaki, X. Zhang, Langmuir 24 (2008) 11988.
[35] G. Sahay, E.V. Batrakova, A.V. Kabanov, Bioconjug. Chem. 19 (2008) 2023.
[36] J.M. Yu, X. Xie, M.R. Zheng, L. Yu, L. Zhang, J.G. Zhao, D.Z. Jiang, X.X. Che, Int. J. Nanomed. 7 (2012) 5079.
[37] T. Thambi, J.H. Park, J. Biomed. Nanotechnol. 9 (2014) 1841.
[38] L.Y. Tang, Y.C. Wang, Y. Li, J.Z. Du, J. Wang, Bioconjug. Chem. 20 (2009) 1095.
[39] Y. Bae, S. Fukushima, A. Harada, K. Kataoka, Angew. Chem. Int. Ed. 42 (2003) 4640.